



Measuring grain rotation at the nanoscale

HPSTAR
401-2017

Xiaoling Zhou^{a,b}, Nobumichi Tamura^b, Zhongying Mi^a, Lingkong Zhang^a, Feng Ke^a
and Bin Chen^a

^aCenter for High Pressure Science and Technology Advanced Research, Pudong, Shanghai, People's Republic of China; ^bAdvanced Light Source, Lawrence Berkeley National Lab, Berkeley, CA, USA

ABSTRACT

In this paper, we introduced a method to measure grain rotation of nanomaterials under external stress using a high pressure diamond anvil cell and the Laue microdiffraction technique at a synchrotron facility. We used tungsten carbide marker crystals to investigate grain rotation activities of 3 and 500 nm nickel media. Our results show that the grain rotation of 3 and 500 nm nickel nanocrystals increase with pressure and finally rotation of 500 nm nickel tends to stop at a lower pressure/stress level than 3 nm nickel. 3 nm nickel nanocrystals show a higher rotation magnitude than 500 nm nickel nanocrystals. Our measurements show an effective method to study the grain rotation of nanomaterials especially in ultrafine nanocrystals.

ARTICLE HISTORY

Received 29 March 2017
Accepted 21 May 2017

KEYWORDS

Diamond anvil cell; laue microdiffraction; grain rotation; deformation; nanomaterials

1. Introduction

Metals and ceramics are aggregates of grains with defined crystalline orientations. The structure and dynamics of grains and grain boundaries are fundamental to the understanding of material deformation properties and has attracted great research interests during the last decades [1–6]. Grain rotation [4,7–18], though not usually considered to be an important mechanism of plastic deformation in bulk-sized materials, has significantly more relevance when applied to nanomechanics. It is believed that below a certain size, grain-boundary-mediated plastic deformation (e.g. grain rotation, grain boundary sliding and diffusion) substitutes for conventional dislocation nucleation and motion as the dominant deformation mechanism in nanomaterials [1–4,16]. However, new findings such as dislocation-mediated plasticity and dislocation activity in ultrafine nanocrystals have been reported, offering a more complex picture of deformation mechanisms at the nanoscale [5,6,19,20]. Thus, investigations on the plastic deformation of nanomaterials, especially the grain rotation behavior, are still urgently needed to uncover the puzzle of plastic deformation at the nanoscale.

Experimental observations of grain rotations are feasible at the micron and sub-micron scale. Grain rotation was first observed in the subgrain growth of cold-rolled metals and alloys during recrystallization [21]. Harris et al. [7] observed the grain rotation of nano gold film during annealing with TEM and predicted that the rotation rate is very

sensitive to the grain size. Margulies et al. [8] studied the grain rotation of micro-sized aluminum sample during tension with 3D X-ray diffraction microscopy (3DXRD) and found that the experimental rotation rates follow the Taylor model well. Murayama et al. [18] observed the disclination dipoles in mechanically milled nanocrystalline Fe powder and suggested that motion of the disclinations along grain boundaries lead to the crystal lattice rotation. Wang et al. [16] studied the deformation-induced grain rotation of nanocrystalline platinum film and suggested that the mechanism underlying the grain rotation is dislocation climb at the grain boundary rather than grain boundary sliding or diffusional creep.

However, the results in these previous studies only offer a partial answer because of the statistical limitation of TEM observations and the low spatial resolution of the X-ray diffraction technique. The question of whether grain rotation rate is significantly depending on grain size has not yet been answered by experimental evidence. Detecting grain rotation of nanomaterials, especially in ultrafine nanocrystals, is still an experimental challenge. In this work, we proposed a method to measure grain rotation of ultrafine nanocrystals by using synchrotron Laue microdiffraction and *in situ* high pressure diamond anvil cell (DAC) techniques. Since the sub-10 nm beam is not yet available and the signals from individual nano grains are too weak to be detected with XRD, the signal from the marker grains are measured instead. Rotation of specific hard marker grains with larger sizes is used as proxies to infer grain rotation inside the nanocrystalline medium. The candidate tungsten carbide (WC) grains, with a high yield strength and consisting of heavy atoms for a good X-ray signal, have been selected as the markers. The methodology has been successfully applied to the investigations of 3 and 500 nm nickel nanocrystals.

2. Experiment

The sample was prepared by mixing high-purity WC powder with an average size of 6–8 μm with 3 and 500 nm Ni powder (Figure 1) with a molar ratio of 1:9, respectively. The mixture was stirred for 2 h using high-energy ultrasonic stirring with alcohol in a sealed bottle. A bit of the dried sample was randomly chosen to test with synchrotron X-ray diffraction characterization and to check whether WC grains were included in the small amount of the sample.

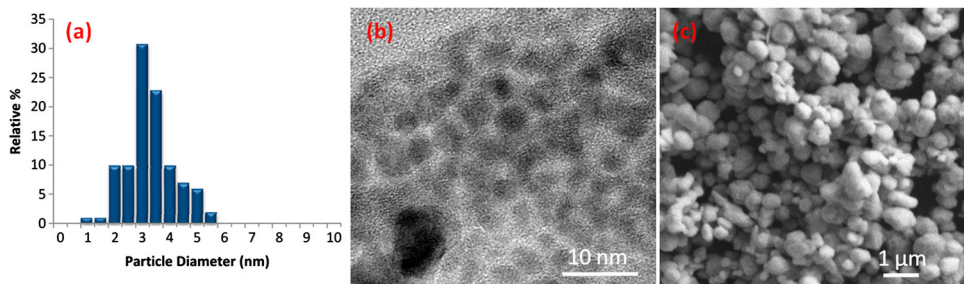


Figure 1. (a) Particle size distribution of 3 nm nickel (Image courtesy of nanoComposix); (b) TEM image of 3 nm nickel; (c) SEM image of 500 nm nickel.

High pressure was generated using a panoramic-type DAC with large openings to allow obtaining maximum angular range for data collection. Boron gaskets with a chamber of $60 \times 80 \mu\text{m}$ filled in a plastic captain was used to avoid the signal of gaskets [22]. The mixture powder of nano nickel medium and embedded WC marker grains was pre-compressed to thin chips before loading into the chamber of DAC. In order to maximize the deviatoric stress on the samples, no pressure medium was used. Ruby was used as a pressure calibrant. High pressure Laue microdiffraction measurements were performed at beamline 12.3.2 of the Advanced Light Source (ALS), Lawrence Berkeley National Laboratory, USA. The incident white beam illuminated the sample from the axial direction and the reflections of sample were collected from the radial direction. This geometry proves to be optimal for collecting the maximum number of Laue reflections (Figure 2, left). The white beam size was tuned to be $2 \mu\text{m} \times 2 \mu\text{m}$, which enable the collection of Laue spots of 6–8 μm WC grains.

At each pressure value, the sample was raster-scanned under the beam with a 2 μm step size and a Laue pattern was collected at each scan step using a DECTRIS Pilatus 1 M hybrid pixel detector placed above, the DAC at an angle of 90° with respect to the incoming beam (Figure 2, left). The diffraction experiment was performed through the diamonds. The series of Laue patterns taken at each pressure step were analyzed using the X-ray Microdiffraction Analysis Software (XMAS) [23]. The diamond reflections were digitally subtracted from the pattern to allow the indexing of the weaker WC Laue reflections.

3. Results and discussions

As shown in Figure 2 (right), a collected raw pattern of WC and diamond anvil can be seen. We indexed the large strong spots of the two diamond anvils first and then masked these spots before indexing WC marker grains. The experimental geometry parameters were precisely refined using the Laue indexing from the two diamond anvils. Signals of

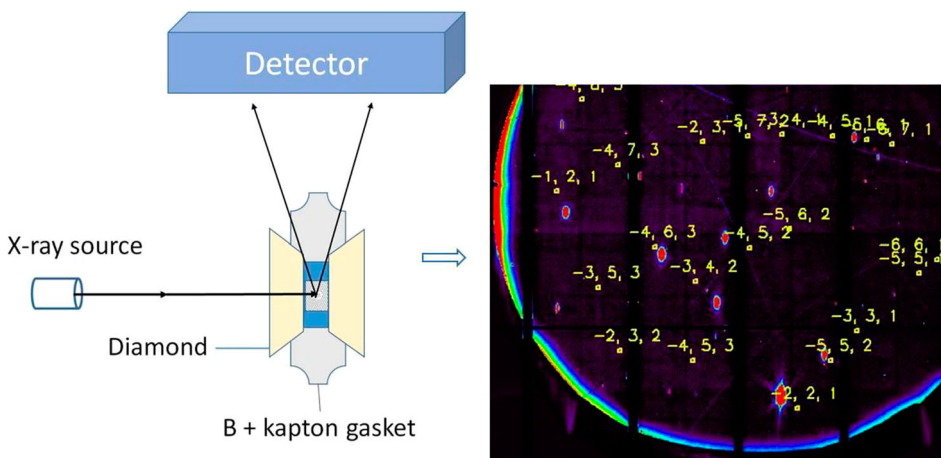


Figure 2. Left: Experimental set-up of high pressure Laue X-ray microdiffraction. Right: indexed Laue pattern of one WC grain embedded in 3 nm nickel.

nickel medium were not found in the patterns because of the weak reflections resulting from the nanoscale grains as well as the overlapping of the Laue patterns of the multitude of illuminated grains contributing only to as a continuous background signal on the detector. A confidence level for the indexation is given by having at least eight spots for the hexagonal structure indexed for each grain. The successful indexation of the WC grains provide an orientation matrix for each of them. The rotation angle of the marker grain can be quantitatively calculated in the XMAS software by inputting the two orientation matrix at different pressures.

The big challenge in this work was to track the same grain in the chamber under different pressures, as grain not only rotate but may also move during compression. It was resolved by raster scanning the whole sample chamber with the X-ray beam, to map all grains embedded in the Ni medium at a given pressure, and using small pressure increment of 0.5–1 GPa. Figure 3 (a–d, f–i) shows the maps of average background, sum peak intensity, number of indexed WC peaks and orientations of WC crystals embedded in 3 nm nickel medium at 0.7 GPa and 1.5 GPa. Each pixel on the maps corresponds to one collected Laue pattern. We checked the patterns around the same relative positions and the same or similar patterns were attributed to be derived from the same marker grain. As shown in Figure 3(e, j), the two patterns are similar but the positions of their spots are different. They derived from the same marker but with different orientations. The shifting of peak positions of a given grain relative to the diamond result from orientation changes under pressure and is used to calculate grain rotation. The change in peak shape is linked to intragranular dislocation activity.

Figure 4 shows 2D crystal orientation maps of WC marker embedded in 3 nm nickel at different pressures. The different colors of the neighboring pixels reflect the polycrystalline nature of the sample aggregates and the overlapping of their positions in 2D projection maps. The subtle color changes of the same grains at different pressures indicated that

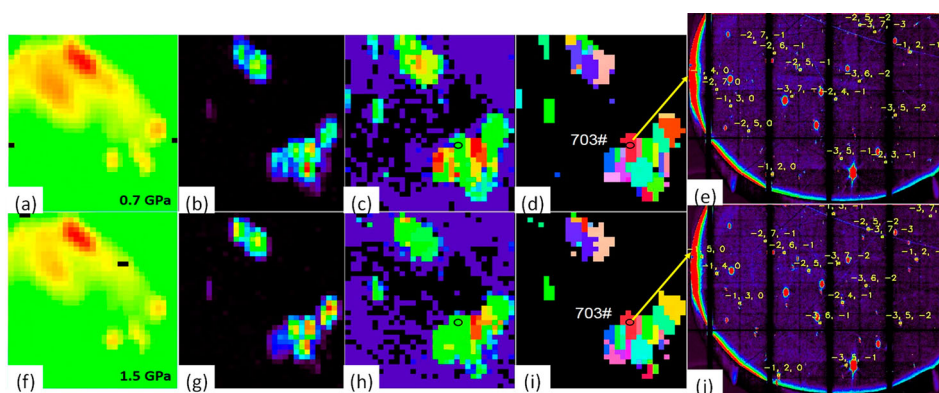


Figure 3. Distribution of average background, sum peak intensity, number of indexed WC peaks and orientations of WC crystals in 3 nm nickel medium at 0.7 GPa (a–d) and 1.5 GPa (f–i). (e, j) are collected Laue patterns of the same WC crystal at 0.7 GPa and 1.5 GPa, respectively. The red and black colors in the background and peak intensity maps indicate the maximum and minimum intensity, respectively. They indicate the maximum and minimum number of indexed peaks in Figure 2(c, h) but indicate different orientations in the orientation maps.

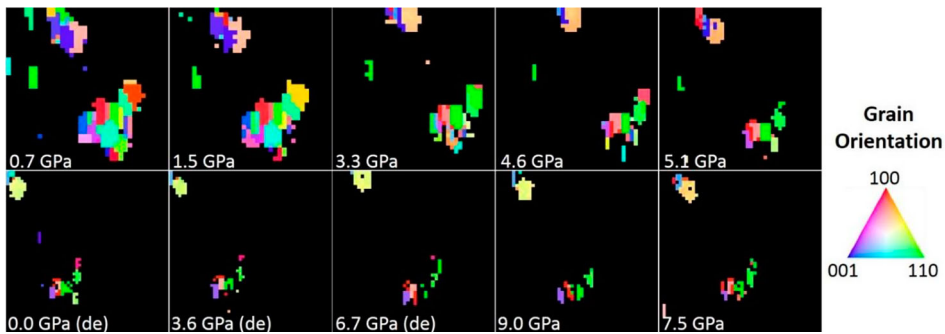


Figure 4. 2D crystal orientation maps of WC marker embedded in 3 nm nickel at different pressures.

the grains rotate under external stress. Under the effect of external pressure, some grains appear or disappear on the maps due to the movement of grains in three dimensions. There are also some apparent ‘disappearance’ of grains on the maps, due to the difficulty to automated index broadened reflections at high pressure. These ‘missing’ grains can still be manually found and tracked around their relative positions.

We took one WC marker grain embedded in 500 nm nickel medium as an example to show the evolutions of the spot at different pressures (Figure 5). The large strong spot of diamond anvil can be referenced for the observation of grain rotation. The position of the WC $(-5,3,-2)$ reflection shifts relative to the position of diamond spot $(-1,7,-1)$ with pressure, indicating the marker grain rotates. However, the relative position changes very slightly above 5.5 GPa and during decompression, suggesting that the grain rotation almost stopped possibly due to greatly reduced mobility at high pressure. The intensity of the WC spot decreased with increased pressure, due to multiple effects, such as increased micro strain and dislocations.

Figure 6 shows the plots of rotation angles of WC marker grains with pressure in different nickel media. The rotation angle is calculated by comparing the orientation matrix at high pressure with the one obtained at the lowest pressure (~ 0.7 GPa). Marker grains are suggested to rotate as the pressure increased and finally tend to stop at high pressure in 500 nm nickel due to the greatly reduced mobility. The rotation magnitude of WC marker grains embedded in 500 nm nickel medium is of 1° – 3° , which is consistent with the results of bulk aluminum specimen in the previous studies [8,11]. The marker grains embedded in 3 nm nickel tend to have a much higher rotation angle than those that are embedded in 500 nm nickel. Since the marker grains are the same, the difference in the different rotation are thus expected to originate from the rotation activity of nano nickel medium, *i.e.* 3 nm nickel exhibits a higher rotation magnitude than 500 nm nickel.

The proposed grain rotation mechanism in previous studies can be classified into two basic types of models: rigid rotation model caused by grain boundary dislocation and grain shearing model caused by dislocation gliding across the grains [24]. The grain boundary dislocation-mediated grain rotation model is widely supported by most simulations [14,25,26] and observations [16,25,27] in the plastic deformation of metals. In this model, grain boundary dislocation can be resolved as an edge component normal to the grain boundary plane and two screw components parallel to the grain boundary plane. With the effect of external shear stress, the edge component causes the displacement of dislocation in the direction normal to the grain boundary and the concurrent

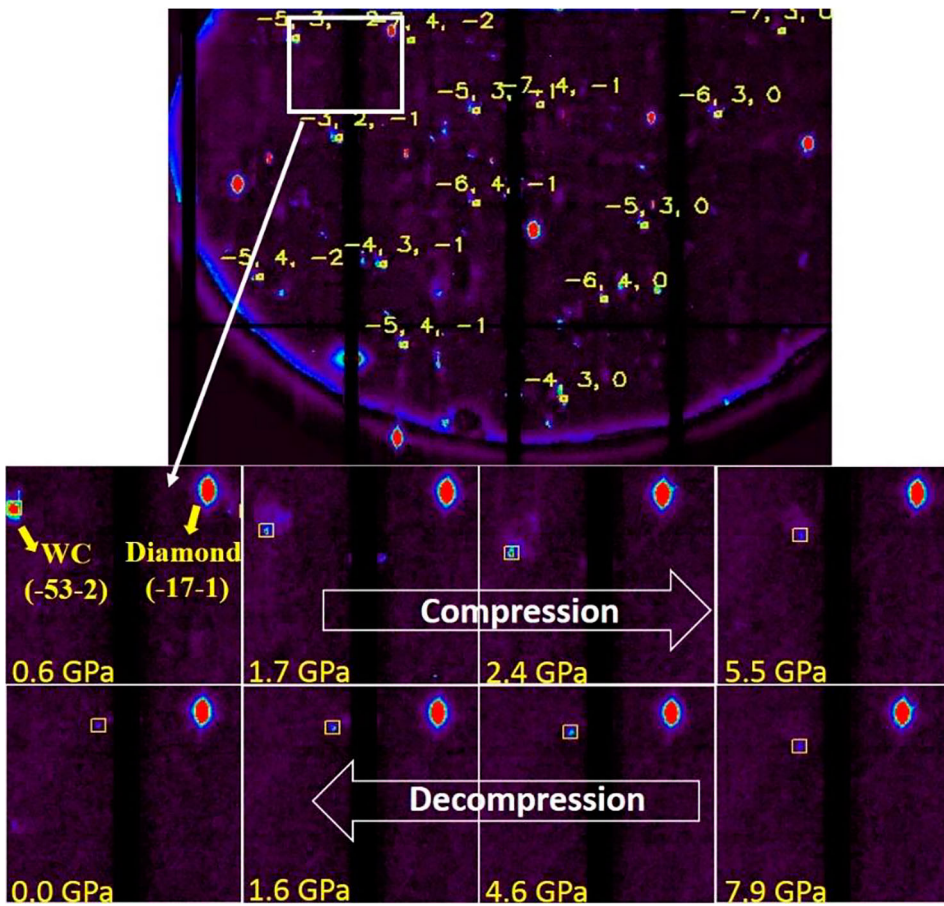


Figure 5. Evolutions of a tracked WC spot (-53-2) embedded in 500 nm nickel at different pressures. The centroid coordinates of all cutoffs are 414 and 92 with a zoom factor of 2.

displacement of the two screw components in the same direction produces the two perpendicular shears and causes grain rotation [25]. Another model, the grain shearing model, is supported by the formation of texture in the plastic deformation of bulk-sized polycrystals [8]. In this model, external force produces dislocations within the lattice and the movement of dislocation causes the lattice planes sliding along certain directions (slip directions) within certain planes (slip planes), resulting in the shape change of the crystal. To achieve the stress equilibrium at grain boundary, the grains rotate and change their crystallographic orientations forming the deformation texture. However, grain shearing model is usually believed to be not operative especially in the rotation of nanomaterials due to the lack of evidence on grain interior slips [16,24,28]. In recent updated experimental findings [17,20], grain interior dislocations are found to be active down to 3 nm, providing a support for the reasonability of the grain shearing model. In addition, the observed reversal in the size dependence of grain rotation further proves that both grain boundary dislocation-mediated model and grain shearing model contribute to the stress-driven rotation of nanocrystals [17]. In our experimental range (<9 GPa), no grain interior slips were found in 3 nm nickel, whereas a lot of slips were observed in

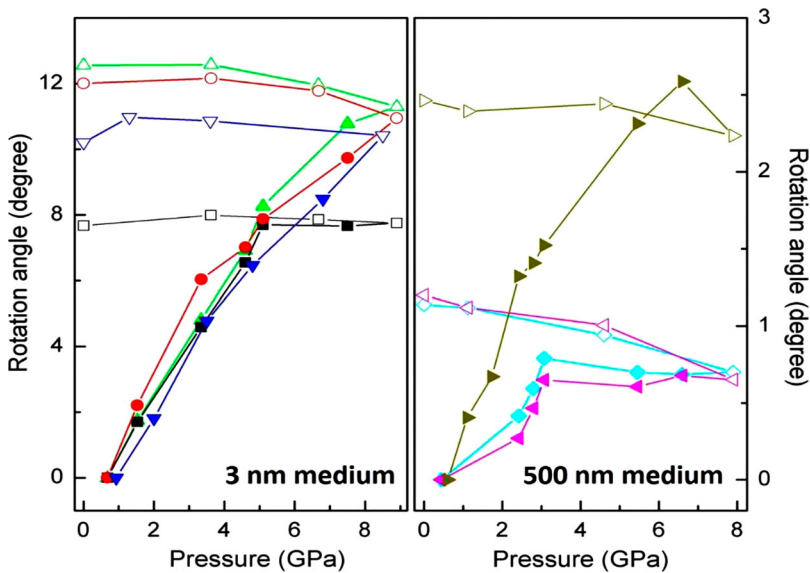


Figure 6. Rotation angles of WC marker grains vs. pressure.

500 nm nickel [17,20]. In this case, it is possible to infer that the dominant model are grain boundary dislocation shearing and grain interior dislocation shearing in 3 nm and 500 nm nickel, respectively. However, it is still unclear whether other mechanisms may also play a role in influencing grain rotation.

Admittedly, the indirect measurements may give underestimations on the rotation of single grain since the marker grains reflect the combined effects of the interactions of numerous nano grains. However, it is difficult to find other techniques to study grain rotation of ultrafine nanocrystals. Sub-10 nm 3DXRD with sub-10 nm depth resolution and high pressure TEM techniques are not yet available, and it is also difficult to track nano grains at different pressures since a large quantity of nano grains will be illuminated considering the high penetration depth of X-ray beam. Therefore, our method provides an effective way to study grain rotation of nanomaterials especially in ultrafine nanocrystals.

4. Conclusions

We successfully used WC marker crystals to reflect the grain rotation activity of 3 nm and 500 nm nickel nanocrystals by using in situ high pressure DAC and synchrotron Laue microdiffraction. The grain rotation of 3 nm and 500 nm nickel nanocrystals increase with pressure and tend to saturate at a lower pressure/stress level in 500 nm nickel. Moreover, 3 nm nickel nanocrystals show a higher rotation magnitude than 500 nm nanocrystals. Our measurements show an effective method to study grain rotation of nanomaterials especially in ultrafine nanocrystals.

Acknowledgements

This research used resources of the Advanced Light Source, which is a DOE Office of Science User Facility under Contract No. DE-AC02-05CH11231.

Disclosure statement

No potential conflict of interest was reported by the authors.

Funding

The authors acknowledge the support of NSAF (Grant No. U1530402). X. Z. was partially supported by the ALS Doctoral Fellowship in Residence Program.

References

- [1] Yamakov V, Wolf D, Phillpot SR, et al. Dislocation processes in the deformation of nanocrystalline aluminium by molecular-dynamics simulation. *Nat Mater*. 2002;1:45–49.
- [2] Shan Z, Stach EA, Wiezorek JM, et al. Grain boundary-mediated plasticity in nanocrystalline nickel. *Science*. 2004;305:654–657.
- [3] Budrovic Z, Van Swygenhoven H, Derlet PM, et al. Plastic deformation with reversible peak broadening in nanocrystalline nickel. *Science*. 2004;304:273–276.
- [4] Chen B, Lutker K, Lei J, et al. Detecting grain rotation at the nanoscale. *Proc Natl Acad Sci*. 2014;111:3350–3353.
- [5] Kumar KS, Suresh S, Chisholm MF, et al. Deformation of electrodeposited nanocrystalline nickel. *Acta Mater*. 2003;51:387–405.
- [6] Chen M, Ma E, Hemker KJ, et al. Deformation twinning in nanocrystalline aluminum. *Science*. 2003;300:1275–1277.
- [7] Harris KE, Singh VV, King AH. Grain rotation in thin films of gold. *Acta Mater*. 1998;46:2623–2633.
- [8] Margulies L, Winther G, Poulsen HF. In situ measurement of grain rotation during deformation of polycrystals. *Science*. 2001;291:2392–2394.
- [9] Moldovan D, Wolf D, Phillpot S. Theory of diffusion-accommodated grain rotation in columnar polycrystalline microstructures. *Acta Mater*. 2001;49:3521–3532.
- [10] Moldovan D, Yamakov V, Wolf D, et al. Scaling behavior of grain-rotation-induced grain growth. *Phys Rev Lett*. 2002;89:206101.
- [11] Poulsen HF, Margulies L, Schmidt S, et al. Lattice rotations of individual bulk grains. *Acta Mater*. 2003;51:3821–3830.
- [12] Winther G, Margulies L, Schmidt S, et al. Lattice rotations of individual bulk grains part II: correlation with initial orientation and model comparison. *Acta Mater*. 2004;52:2863–2872.
- [13] Weissmüller J, Markmann J. Deforming nanocrystalline metals: New insights, new puzzles. *Adv Eng Mater*. 2005;7:202–207.
- [14] Cahn JW, Mishin Y, Suzuki A. Coupling grain boundary motion to shear deformation. *Acta Mater*. 2006;54:4953–4975.
- [15] Wang YB, Li BQ, Sui ML, et al. Deformation-induced grain rotation and growth in nanocrystalline Ni. *Appl Phys Lett*. 2008;92:011903.
- [16] Wang L, Teng J, Liu P, et al. Grain rotation mediated by grain boundary dislocations in nanocrystalline platinum. *Nat Commun*. 2014;5:4402. DOI:10.1038/ncomms5402
- [17] Zhou X, Tamura N, Mi Z, et al. Reversal in the size dependence of grain rotation. *Phys Rev Lett*. 2017;118:096101.
- [18] Murayama M, Howe JM, Hidaka H, et al. Atomic-level observation of disclination dipoles in mechanically milled, nanocrystalline Fe. *Science*. 2002;295:2433–2435.
- [19] Li X, Wei Y, Lu L, et al. Dislocation nucleation governed softening and maximum strength in nano-twinned metals. *Nature*. 2010;464:877–880.
- [20] Chen B, Lutker K, Raju SV, et al. Texture of nanocrystalline nickel: probing the lower size limit of dislocation activity. *Science*. 2012;338:1448–1451.
- [21] Li JCM. Possibility of subgrain rotation during recrystallization. *J Appl Phys*. 1962;33:2958–2965.
- [22] Merkel S, Yagi T. X-ray transparent gasket for diamond anvil cell high pressure experiments. *Rev Scient Instrum*. 2005;76:046109.

- [23] Tamura N. XMAS: a versatile tool for analyzing synchrotron X-ray microdiffraction data. London: Publisher; 2014.
- [24] Upmanyu M, Srolovitz DJ, Lobkovsky AE, et al. Simultaneous grain boundary migration and grain rotation. *Acta Mater.* 2006;54:1707–1719.
- [25] Gorkaya T, Molodov KD, Molodov DA, et al. Concurrent grain boundary motion and grain rotation under an applied stress. *Acta Mater.* 2011;59:5674–5680.
- [26] Ivanov VA, Mishin Y. Dynamics of grain boundary motion coupled to shear deformation: An analytical model and its verification by molecular dynamics. *Phys Rev B.* 2008;78. DOI:10.1103/PhysRevB.78.064106
- [27] Gorkaya T, Molodov DA, Gottstein G. Stress-driven migration of symmetrical $\langle 100 \rangle$ tilt grain boundaries in Al bicrystals. *Acta Mater.* 2009;57:5396–5405.
- [28] Kobayashi R, Warren JA, Carter WC. A continuum model of grain boundaries. *Physica D: Nonlinear Phenomena.* 2000;140:141–150.